Journal of Environmental Management 392 (2025) 126644

Contents lists available at ScienceDirect

Journal of Environmental Management

journal homepage: www.elsevier.com/locate/jenvman

Research article

From coal ash to the nuclear fuel cycle: A new method of uranium extraction with membranes

Filip Jedrzejek [a,*], Weronika Mendera [a], Katarzyna Szarlowicz [a], Niklas Heiss [b], Ulrich W. Scherer [b]

[a] AGH University of Krakow, Faculty of Energy and Fuels, Mickiewicza 30, Krakow, 30-059, Poland
[b] Technical University Mannheim, Institute of Physical Chemistry and Radiochemistry, Paul-Wittsack-Str. 10, Mannheim, D-68163, Germany

ARTICLE INFO

Keywords:
Uranium extraction
Coal combustion by-products
Nuclear fuel cycle
Sustainable nuclear energy

ABSTRACT

This study presents results from experiments on uranium leaching from coal combustion through theproducts by use of a membrane system. The aim of the study was to develop a basic operational model for a novel system dedicated to dusty materials that form colloids and are difficult to separate. Experiments were conducted to evaluate the efficiency and rate, along with the dynamics of uranium diffusion through the membrane. The results indicate that the proposed method allows efficient uranium leaching, with an average yield of 96.7 %. To describe the process, kinetic models were applied: second-order reaction kinetics for the leaching step and simple diffusion for uranium transport through the membrane. This membrane-assisted approach effectively addresses the challenges posed by the complex physical nature of ash residues, and its further refinement may enhance the efficiency of the process and support the principles of circular economy within the nuclear fuel cycle. Key experimental parameters, including the permeability coefficient and the leaching rate constant, were determined and will serve as the basis for the design of operations in subsequent stages of industrial application. The proposed membrane approach solves the problematic issues related to the difficult form of ashes, and further development can lead to optimisation of the fuel cycle in modern power generation.

1. Introduction

Uranium is a major global resource for nuclear energy and is the cornerstone of sustainable energy production and the mitigation of climate change. As the primary fuel for nuclear reactors, uranium facilitates the generation of substantial amounts of electricity through the process of nuclear fission, resulting in significantly lower greenhouse gas emissions compared to fossil fuels. These attributes establish nuclear energy as an essential component in the global transition towards a low carbon economy, contributing to the reduction of the environmental impact associated with energy production and addressing global warming (Edenhofer O and Sokona, 2011; Harrison, 2018; Intergovernmental Panel on Climate, 2015). The high energy density of nuclear power indicates that a small quantity of uranium can produce a considerable amount of energy, making it an efficient and sustainable option to meet the burgeoning global energy demands (IAEA, 2023; Muellner et al., 2021; Peters et al., 2018). Within the framework of sustainable development, the efficient and responsible stewardship of uranium resources is of utmost importance.

The principal methods of uranium extraction involve either underground mining or open-pit mining. Determining the optimal mining system for a specific deposit can be exceedingly intricate, necessitating the consideration of numerous factors such as ore depth, deposit size, ore grade, ground conditions, surface topography, etc. Traditional mining practices pose environmental and safety challenges, thus underscoring the significance of advanced methodologies such as in situ recovery (ISR) and bioleaching, which mitigate ecological impact and promote safety (Saunders et al., 2016). The integration of circular economy principles, such as the recycling of spent nuclear fuel and the recovery of uranium from waste, can mitigate resource depletion and minimize environmental damage (Gao et al., 2023; Verma and Loganathan, 2025). These strategies support the objectives of sustainable energy production, climate targets, and resource efficiency (NEA, 2014).

A conceivable source of uranium may be found in the waste materials produced by the combustion of coal in power plants. The uranium present in fossil fuels and their combustion products potentially offers a

* Corresponding author. AGH University of Krakow, Faculty of Energy and Fuels, al. Mickiewicza 30, Krakow, 30-059, Poland.
E-mail address: jedrzejek@agh.edu.pl (F. Jedrzejek).

https://doi.org/10.1016/j.jenvman.2025.126644
Received 18 March 2025; Received in revised form 4 July 2025; Accepted 16 July 2025
Available online 25 July 2025

substantial quantity of valuable raw material suitable for nuclear fuel production. Quantitative data related to these materials are provided in Table 1.

There is notable variability in uranium concentrations, attributed both to the geochemical processes operating during the formation of deposits and to the mechanisms responsible for the concentration of trace elements during coal combustion. As a high-atomic weight element, uranium preferentially accumulates in environments characterised by specific geochemical conditions, including clay deposits, peat bogs, or regions influenced by hydrothermal fluids (Finkelman, 1994; Zielinski and Finkelman, 1997). The uranium content in lignite and bituminous coal exhibits marked differences, which can be ascribed to their distinct geological origins, varying degrees of coalification, and mineral compositions. As a result of their relatively recent age and lower degree of carbonisation, lignite coals possess a higher abundance of organic matter and clay minerals, enabling the efficient absorption of uranium from groundwater and hydrothermal vents. Their development in swamp and peatland environments has promoted the concentration of this element under reducing conditions, as uranium remains mobile in oxidising environments. Under anaerobic conditions, it can precipitate and associate with organic matter and clay minerals (Zielinski and Finkelman, 1997). Bituminous coal, as a more advanced stage of coal maturation, exhibits a reduced content of volatile elements and an elevated elemental carbon content, which constrains its ability to incorporate uranium within its organic structure. Consequently, uranium within bituminous coals exists predominantly in a mineralized form, associated with clay admixtures, phosphates, and iron sulphides. Localised enrichment may occur due to hydrothermal mineralisation, particularly in deposits exposed to subsequent geochemical processes such as mineral recrystallisation or trace element remobilization (Hower et al., 1999).

Table 1
The uranium content of fossil fuels and their combustion products.

Material	Country	Uranium concentration [mg/kg]	
Lignite	Greece	9,4–31,3	IAEA (2003)
	Italy	1,6–2,0	IAEA (2003)
	Serbia	2,2–5,7	Životić et al. (2008)
	Russia	1,7	Arbuzov et al. (2011)
	Australia	1,6	Vance (2016)
Bituminous coal	Poland	0,1–12,8	(IAEA, 2003; Olkuski, 2008; Smolka-Danielowska, 2010; Walencik-Łata and Smołka-Danielowska, 2020)
	USA	0,5–5,9	IAEA (2003)
	Australia	0,7–3,8	IAEA (2003)
	Brazil	5,8	IAEA (2003)
	Egypt	4,7	IAEA (2003)
	Romania	0.1–3,4	IAEA (2003)
	UK	0,6–1,5	IAEA (2003)
	Russia	1,3–4,5	(Arbuzov et al., 2011; IAEA, 2003)
	Kazakhstan	<1	Arbuzov et al. (2011)
	Mongolia	1,5	Arbuzov et al. (2011)
	RPA	1,9–3,2	Ahmed et al. (2020)
	China	0,8–450,1	IAEA (2015)
Fly ashes	USA	7,7–30,0	(IAEA, 2003; Zielinski and Finkelman, 1997)
	UK	3,5–8,8	IAEA (2003)
	Croatia	699,2	IAEA (2003)
	Brazil	11,6	IAEA (2003)
	Serbia	8,0–14,0	Životić et al. (2008)
	Poland	0,2–19,2	(Smolka-Danielowska, 2010; Walencik-Łata and Smołka-Danielowska, 2020)
	Vietnam	5,4–10,3	IAEA (2015)
	India	3,1–10,2	(Mahur et al., 2008; Walencik-Łata and Smołka-Danielowska, 2020)
Bottom ashes and slags	Poland	6,8	Walencik-Łata and Smołka-Danielowska (2020)
	Brazil	12,5	IAEA (2003)
	Croatia	273,2	IAEA (2003)
	USA	2,1	IAEA (2003)
Unqualified ashes	Poland	5,4–11,3	Walencik-Łata and Smołka-Danielowska (2020)
	Turkey	11,5–38,0	Walencik-Łata and Smołka-Danielowska (2020)
	Serbia	0,33–11,5	Životić et al. (2008)
	China	250	Vance (2016)

In contrast to unprocessed coal, the by-products of its combustion, particularly fly ash, slag, and bottom ash, exhibit significantly elevated concentrations of uranium (Mishra et al., 2023). This phenomenon arises from the combustion process, in which volatile elements such as carbon, hydrogen and sulphur undergo oxidation, while elements with higher boiling points, such as uranium, persist in the solid phase and become concentrated within the mineral residues (Monnet et al., 2015; Nian, 2016). The by-product may serve as an effective source of uranium; however, a considerable challenge in extracting uranium from dust-laden waste (e.g. coal combustion ash) is its nonmorphic nature, which leads to the formation of suspensions when acid solutions interact with the ashes (Karamanis and Vardoulakis, 2012).

The uranium leaching procedure is intricate and demanding; however, considering the significance and potential utility of fly ash, initiatives were undertaken to develop a new procedure for extracting uranium from this by-product. To ameliorate separation challenges, this study introduces an innovative approach utilising semipermeable membranes within the procedure. This concept fits within broader environmental and circular economy strategies, as many coal combustion residues are historically deposited in landfills or slag heaps, particularly in postindustrial and former mining regions. These areas, often in need of environmental remediation, may become potential sites for resource recovery. Efficient recovery of strategic elements these as uranium from such waste streams could contribute to the revitalisation of these areas and support national and international decarbonisation goals.

In order to improve the extraction, it is crucial to understand the processes of uranium recovery from coal ash. The leaching of uranium from coal ash in a semi-permeable membrane system involves a series of interconnected processes. Initially, the solvent interacts with the coal ash, dissolving the uranium species present on its surface. This dissolution is influenced by oxidation reactions, which determine the solubility of uranium compounds and facilitate their release into the liquid phase. Subsequently, the solvent penetrates the porous structure of the coal ash, enabling the dissolution of uranium trapped deeper within the material. Once the uranium ions are dissolved, they are distributed in the leaching agent solution, driven by diffusion forces (Richardson et al., 2002). At this stage, the typical leaching process ends. However, in the case of fly ash, which is a fine-grained material, the result is the formation of a uranium-rich colloid that is difficult to separate (Delegard and Schmidt, 2009; Karamanis and Vardoulakis, 2012; Su et al., 2014). In the proposed system, the resulting suspension is separated by a membrane from the actual cell from which the uranium is collected for the subsequent extraction procedure. The membrane plays a crucial role by permitting the selective passage of uranium ions while retaining larger particles or impurities. This step involves diffusion through the membrane, where the solute moves under a concentration gradient or pressure-driven mechanism to the collection side for recovery or further processing. However, this affects the kinetics of the process and introduces these further steps.

In essence, the membrane acts as a filter and enables the separation of particulate ash matter from the liquid phase containing uranium ions. It simplifies the extraction process by resolving issues associated with suspended solids that can impede conventional recovery techniques. The entire procedure requires the optimisation of each step in uranium

extraction; therefore, the primary objective of the project was to investigate the kinetics of the leaching reaction, including the transport of uranium ions through the semipermeable membrane. To achieve this, gamma-ray spectrometry was employed to determine the radioactivity of materials and, consequently, calculate the uranium content. A liquid scintillation counter was utilised to assess the uranium leaching rate constant and uranium permeability in the diffusion process. This approach was intended to acquire critical design parameters essential for the further development of the method.

2. Materials and methods

2.1. Raw material characteristic

A fly ash sample was obtained taken from the electrostatic precipitator of a coal-fired power plant. The sample was homogenised and sieve with a mesh size of 125 μm.

The total uranium content of the ash and its isotopic characteristics were determined by analysis of the emitted gamma-rays using a spectrometer with HPGe detector (Mirion, model BE3830). The system was equipped with lead shielding (LS1112) and a background reduction feature (Jędrzejek and Szarłowicz, 2024). Calibration measurements were performed experimentally with certified reference materials, applying corrections for self-absorption.

The raw ash sample was divided by the quartering method to measurement geometry volume - a cylindrical container with a volume of 27 cm^3. Samples after packaging were measured after 3 weeks, to establish an equilibrium between ^{226}Ra and its progeny, the measurement time was approximately 72 h. Radioactivity of isotope ^{238}U was determined by photopeaks: 92.38–92.80 keV; 63.3 keV and 1001.02 keV, while ^{235}U was determined by 143.76 keV and 185.72 keV. For the energy of 185.72 keV, which represents a doublet together with ^{226}Ra, a correction was applied according to the formula proposed by Y. Ebaid (2015). In other places, detailed descriptions with the energy characteristics of the gamma ray quantum for other isotopes are described (Jędrzejek et al., 2022; Stobiński et al., 2018).

2.2. Uranium extraction

First, the raw ash sample was divided by the quartering method to obtain experimental samples. The leaching condition was adopted from Sun et al. (2016). The samples were then calcined at 900 °C for 2 h with calcium chloride in a 2:1 ratio (ash:$CaCl_2$). After being cooled, the samples were transferred to a glass beaker with a 4 mol dm^{-3} solution of nitric acid (V), continuously stirring. The temperature was kept at 20° throughout the entire experiment. Then, at appropriate intervals, the resulting solution was decanted from the precipitate and, to separate the solution from the ash particles, the suspension was centrifuged at 4000 RPM (t = 10 min). After centrifugation, the precipitate was returned to the beaker, and the supernatant was taken for further analysis. Another aliquot of 4 mol dm^{-3} nitric acid was added to the beaker, to refill to the initial volume of 0.04 dm^3. The procedure was repeated until the solution after centrifugation was completely discolored. Uranium concentration in the supernatant samples was analysed, after prior separation of uranium ions on UTEVA resin (Eichrom Method No: ACW02). After the separation procedure, uranium ions were obtained in a 1 mol dm^{-3} HCl matrice. 0,005 dm^3 of the solution was transferred to a 0.02 dm^3 plastic vial with 0,015 dm3 scintillation cocktail (AquaLight + AB). In addition to this procedure, 4 mol dm^{-3} HNO_3 spiked with a solution of known uranium concentration were prepared in parallel to determine the chemical yield of the procedure (on average 98.30 ± 0.69 %). Uranium activity was determined by liquid scintillation counter LSC and converted to concentration. The uranium concentration was determined by liquid scintillation counter (LSC).

The procedure is summarised in Fig. 1.

2.3. Membrane diffusion process

An experiment of diffusion through a membrane was performed to measure the diffusion rate of uranium ions from liquids separated by a membrane. The experimental design is shown in Fig. 2. The system consisted of two identical cells with a maximum volume of approximately 0.2 dm^3. Between them was a 40 mm diameter hole in which a membrane was placed. The system allowed the membrane to be replaced.

Ultrafiltration membranes (neoLab, Germany) with a molecular weight cut-off point (MWCO) of 14 kDa and a nominal pore size of 3.0–3.5 nm were used. The membranes had a thickness of 0.8 mils (~20 μm) and were composed of a polymeric material functionalised with hydroxyl groups.

First, both cells were filled with deionised water (to a volume of 0.16 dm^3) and then cell 1 was spiked with a solution of known concentration of uranyl acetate of an approximate uranium radioactivity of 5 kBq·dm^{-3}. Then 0.001 dm^3 of solution was taken from cell 2, at the appropriate time regime. The volume of solution was directly added to a vial with 0.01 dm^3 scintillation cocktail (Aqualight + AB). Uranium activity was determined by LSC and converted to concentration. The temperature was kept at 20° throughout the experiment.

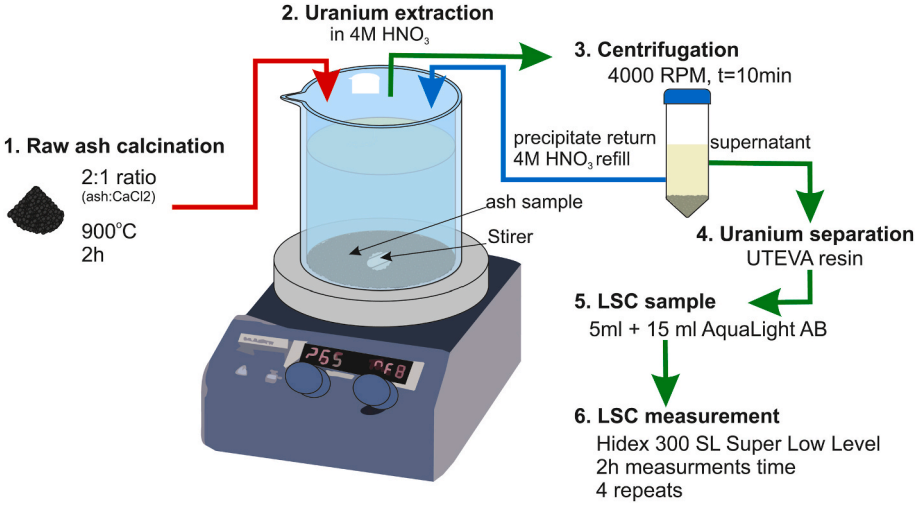

Fig. 1. The analytical procedure of uranium extraction experiment.

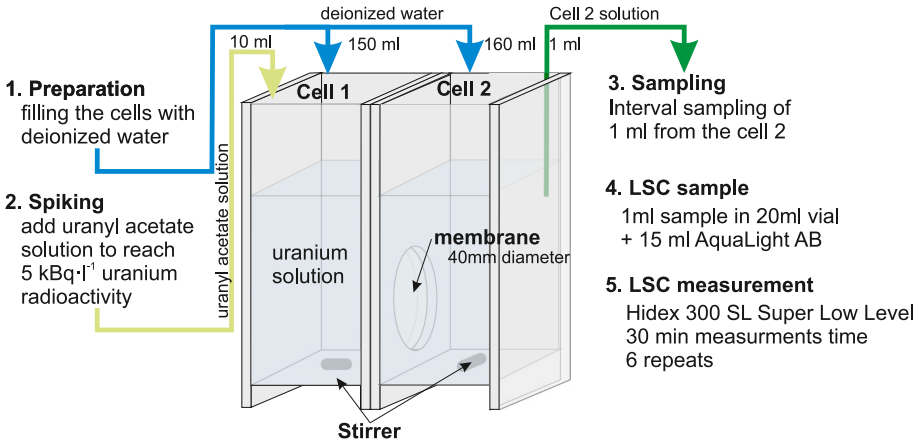

Fig. 2. The analytical procedure of the uranium diffusion process through a membrane.

2.4. Liquid scintillation counting

The samples were measured with a HIDEX liquid scintillation counter, model 300SL Super Low Level. The total uranium concentration was determined by measuring the full spectrum of alpha radiation from isotopes ^{235}U and ^{238}U. For this purpose, the built-in Alpha/Beta separation module was used, selecting the Pulse length index (PLI) to provide the best separation depending on the quenching.

The measurement time was 2 h and 0.5 h for the uranium extraction and membrane diffusion experiments, respectively. The type An uncertainty evaluation was used, taking repeated measurements for each sample.

3. Results and discussion

In this paper, the characterisation of the kinetics of uranium leaching in a membrane system is reduced to two preceding steps: the extraction process of uranium from the raw material and the passage of uranium through the membrane. For practical reasons, the method is divided into two experiments and is described in the following sections.

3.1. Raw material characteristics

First, an analysis was performed to identify the isotopic characteristics of the raw ash and to determine the initial concentration of uranium. The results are summarised in Fig. 3, which in part A shows the concentration of radioactivity of selected isotopes in the raw ash (see Fig. 3A).

The isotope with the highest concentration in the sample was the potassium isotope ^{40}K with a measured activity of 650 ± 10 Bq·kg^{-1}, which significantly exceeding the activity levels of other radionuclides. This is consistent with the natural abundance of potassium and its concentration in fly ash after combustion (Fidanchevski et al., 2021).

The radioactivity of other radionuclides ranged from 129 to 176 Bq·kg^{-1} with ^{226}Ra showing the highest values of 176 ± 5 Bq·kg^{-1}. This result is at the upper limit according to the values reported in the literature for Poland, where the range is from 10.5 ± 0.4 Bq·kg^{-1} to 178 ± 18 Bq·kg^{-1}(Smolka-Danielowska, 2010; Walencik-Łata and Smołka--Danielowska, 2020). A disequilibrium in the uranium-radium series can also be noticed, with increased radium activity in the ash relative to uranium. This has been observed by other authors, already, and is caused by chemical differences between radium and uranium effecting different levels of enrichment during combustion. In addition, within the raw material itself, an equilibrium is rarely observed (Walencik-Łata and Smołka-Danielowska, 2020).

The measured radioactivity of ^{238}U in the fly ash sample was 158 ± 8 Bq·kg^{-1}, indicating a concentration of uranium in the combustion by-product. This value was slightly higher than other data reported for Poland, where the maximum value was 136 ± 10 Bq·kg^{-1}. The activity concentration of ^{235}U was 8.2 ± 1.1 Bq·kg^{-1} and aligns well with the

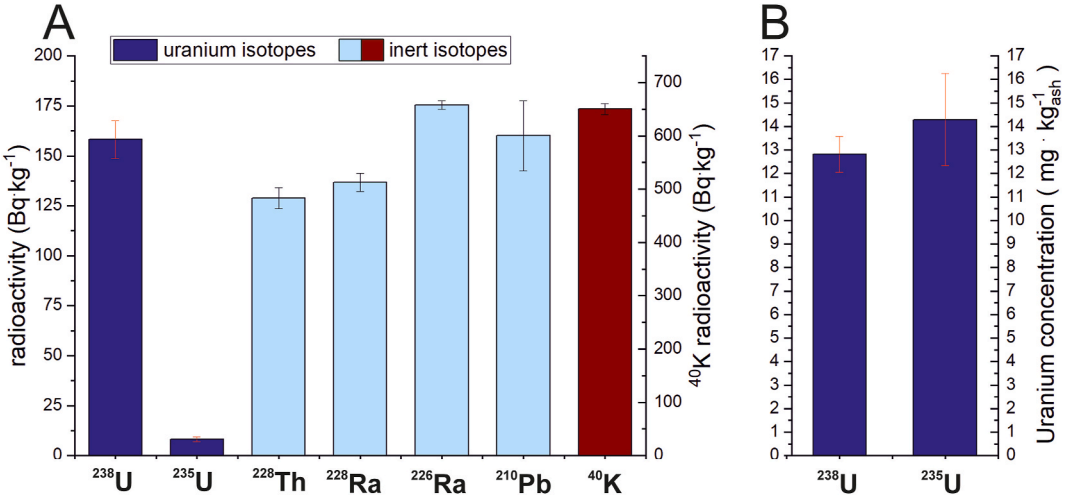

Fig. 3. A. The concentration of radioactivity of selected isotopes in the raw ash; B. the mass concentration of total uranium element, calculated separately from radioactivity of ^{238}U and ^{235}U.

expected natural isotopic ratio of uranium. The $^{235}U/^{238}U$ ratio was 5.1 ± 0.7 %, while the expected value based on natural abundance is 4.6 %. At the assumed confidence level, the values are consistent. This confirms the correct analysis and the reliability of the result.

Fig. 3B shows the mass concentration of total uranium element, calculated from the measured radioactivity of both isotopes. Values are consistent within the uncertainty and the arithmetic mean was taken as the uranium concentration for further analysis, which was 13.6 ± 1.1 $mg{\cdot}kg^{-1}$. Although this value is higher relative to other data reported for Poland, it does not represent any extreme in relation to global values, where for some countries even concentrations as high as 699 $mg{\cdot}kg^{-1}$ are observed (Table 1).

3.2. Dynamics of uranium extraction

The ash leaching experiment was reduced to a practical description of the transition of uranium ions between the solid and liquid phases. Fig. 4A shows the leaching process over time, considering the measured value, that is, the concentration of uranium in the liquid phase. The measured concentration was converted to the total leached uranium and is shown on the graph in Section A. The graph shows the process dynamics as a change in the time of the uranium mass that has been oxidised to the VI - oxidation state and, hence, been transferred to a soluble form. Both samples A and B showed a similar trend in the leaching time path, with slightly higher values for B, especially at the early stages of the process. However, it should be noted that sample B had slightly higher uranium concentration compared to that of sample A, so the difference was expected. The maximum amount of uranium that is possible to get extracted from the ash sample is also shown in the graph.

Data indicate a two-phase leaching process. First, we observe a rapid initial extraction phase, with a steep increase in uranium concentration during the first few hours, suggesting fast oxidation of uranium species and uptake in the leaching solution. This phase probably corresponds to the release of readily available uranium from surface-accessible sites. Second, as time progresses, a gradual plateauing phase is observed. The leaching rate decreases, approaching an equilibrium state in which the extraction process slows significantly. This suggests that the uranium present in more structurally integrated phases requires longer contact times.

Fig. 4B summarises the results of the experiment as a percentage of total uranium leaching. In this case, the data was standardised by the initial uranium amount and presented as total recovery. Both samples exhibit similar leaching behaviour, as evidenced by their nearly identical yields in time intervals. Remarkable is the high average recovery of 96.7 %, indicating the great effectiveness of the applied leaching method.

Based on the results, it can be clearly observed that 50 % of the uranium from e.g. sample B was recovered after about 8 h 45 min, 75 % after 27 h 15 min, and 95 % after 2 days 19 h 45 min. Sample A shows a very similar trend. It suggests that extension beyond a certain threshold yields diminishing returns. This indicates an optimal processing window in which the uranium is extracted efficiently, i.e. the maximum uranium extraction efficiency is reached.

The concentration presented was then used to determine the concentration of uranium in the solid phase, in form of insoluble ions assumed in the +IV-oxidation state.

To determine the kinetics of the leaching process in this system, it was assumed that the primary rate-determining step is the oxidation of uranium. This approach introduces a degree of simplification, potentially underestimating the influence of additional processes, such as impregnation of the ash and penetration of the internal structure by the reactant, diffusion of oxidised uranium from the solid matrix, and equilibration of uranium concentrations in solution. However, given the adopted conditions of the experiment, i.e. intensive mixing and the fine-grained structure of the ash, these effects should be negligible as fast processes. All the mentioned processes are fast compared to oxidation, which can be considered the ‘speed determining’ step. Another assumption was made that uranium was present in coal ash primarily as an oxide. Although uranium may also be present in other forms, such as phosphates, silicates, or aluminosilicates, the use of oxides was the way to simplify the kinetic modelling of the leaching process. A more detailed speciation analysis using techniques such as XRD or XPS could refine the model, but for the purposes of this study, the oxide assumption provides a reasonable approximation of uranium behaviour during leaching and is based on the biogeochemistry of uranium minerals (Taylor, 1979).

The literature study of uranium oxidation by nitric acid showed that there are at least seven different stoichiometric equations, with NO, NO_2, N_2O, N_2, NH_3, NO + NO_2, HNO_2 as products, as summarised by Marc et al. (Fournier, 2000; Herrmann, 1984; Marc et al., 2017).

The oxidation mechanism also remains described in different ways, depending on the approach, e.g., single-electron transfer mechanism, as in the following equations (Berger, 1988).

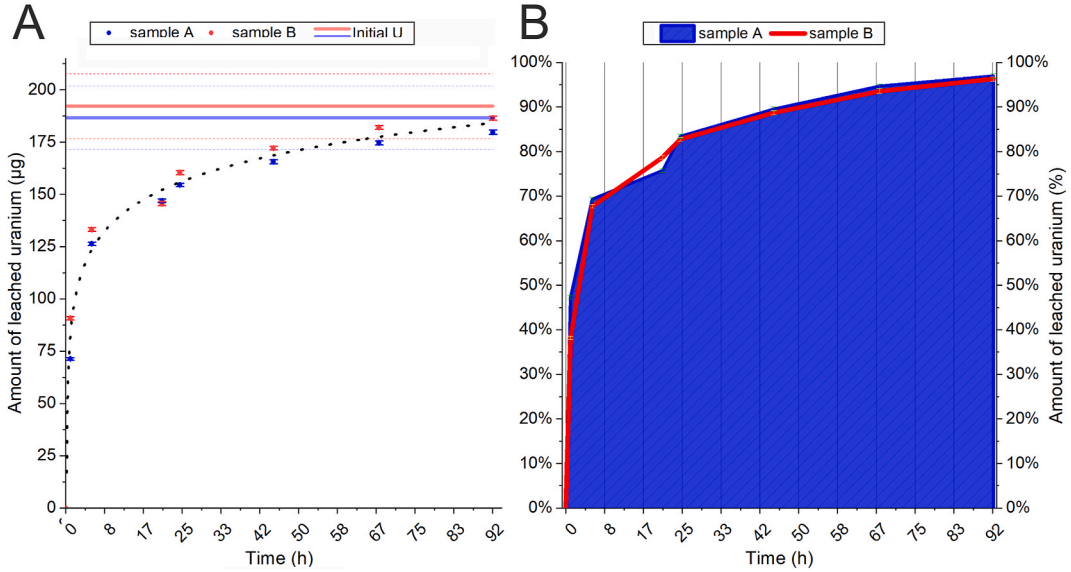

Fig. 4. A- An amount of leached uranium in time intervals; B - Percentage of total uranium over time.

$$UO_{2(s)} = UO^{+}_{2(s)} + e^{-} \quad (1)$$

$$UO^{+}_{2(s)} = UO^{2+}_{2} + e^{-} \quad (2)$$

However, the work of Marc et al. has made a significant contribution to the field by studying all different approaches and claimed that the Ikeda et al. mechanism for a two-electron transfer mechanism is most likely at certain HNO_3 concentrations (Ikeda et al., 1993; Marc et al., 2017). According to this mechanism, the oxidation reaction can be described as follows.

$$UO_2 + NO_3^{-} + 4H^{+} \rightarrow UO^{2+}_{2} + 2NO_2 + 2H_2O$$

The exact stoichiometry and by-products might vary depending on the specific uranium compounds in the coal ash or other minerals present, which also react with nitric acid.

To adopt the kinetics of the reactions and fit the reaction order according to the rate law, the data were examined as shown in Fig. 5. The results shown in the graph represent the average value for all series. Figure part A presents the decrease in U(IV) concentration over time (uranium concentration in ash), where the experimental data were fitted with a nonlinear function (red dashed line). The observed trend suggests progressive uranium oxidation, with a rapid initial decrease followed by a slower decline. This indicates a first- or second-order reaction (see Fig. 5).

Fig. 5B shows the uranium oxidation rate as a function of the U(IV) concentration. The upward curvature of the fitted trend suggests a second-order dependence, where the oxidation rate is proportional to the square of the U(IV) concentration. Mathematically, this follows the rate law:

$$rate = k\left[U^{IV}\right]^2 \quad (3)$$

where k is the second-order rate constant. This result implies that uranium oxidation follows second-order kinetics, where the reaction rate increases significantly at higher uranium concentrations in the ash. The probable reason for this dependence may be a diffusion-limited process in which oxidising agents must penetrate deeper into the solid phase, and available reactive sites decrease as the reaction progresses.

According to second-order kinetics:

$$\frac{1}{\left[U^{IV}\right]} = \frac{1}{\left[U^{IV}\right]_0} + kt \quad (4)$$

where.

t – time.

$\left[U^{IV}\right]$ – uranium concentration in ash at time = t

$\left[U^{IV}\right]_0$ – uranium initial concentration in ash (t = 0)

k – rate constant.

To determine the reaction rate constant k, the data were graphed using eqution (4). The results plotted in the graph represent the average value for all series (see Fig. 6). The graph shows a strong linear relationship with a correlation coefficient of 0.98 and an adjusted Pearson coefficient of 0.95. The equation of the fitted line matches the integrated form of a second-order kinetic equation, where the slope ($3.58.10^{-4} \pm 0.31.10^{-4}$ kg $mg^{-1}{\cdot}min^{-1}$) corresponds to the second-order rate constant. There are some apparent linearity irregularities in the graph, which may be related to the side mechanism of uranium release into solution. Also, the intercept $4.96.10^{-4} \pm 0.084$, which should cover 1 divided by the initial uranium concentration ($1/U_{initial} = 0.073$).

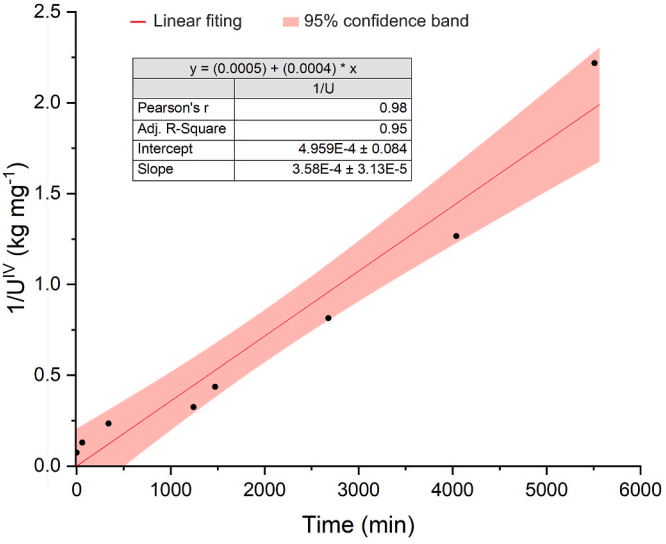

Fig. 6. The dependence of the inverse uranium concentration in the ash over time intervals of oxidation process.

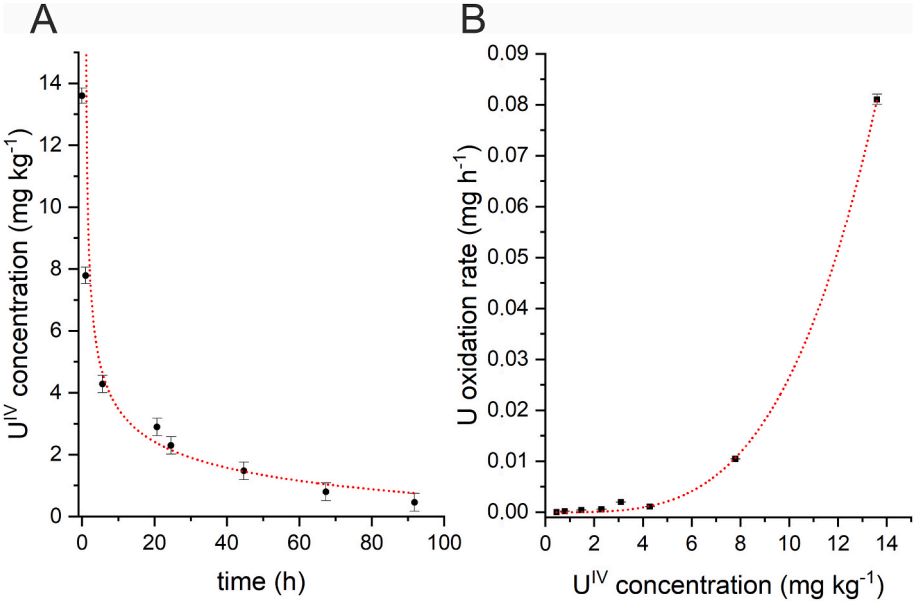

Fig. 5. A - The uranium concentration in ash during the leaching experiment; B - The uranium oxidation rate as a function of the uranium concentration in ash.

Although the intercept falls within the 95 % confidence interval, the relatively high uncertainty suggests that the model does not fully capture the uranium release rate at the very beginning of the process. A likely explanation for this deviation is the presence of uranium already in the oxidised state (U^{VI}) in the raw fly ash. Uranium in this form is highly soluble in nitric acid and may dissolve rapidly during the first moments of leaching, leading to an initial concentration increase not strictly by the surface oxidation mechanism assumed in the model. This phenomenon could be further supported by the possibility of partial oxidation of uranium during a prior thermal treatment (calcination). However, the general good correlation confirms that uranium removal follows a reaction-controlled mechanism.

Therefore, in practical applications, the second-order kinetics equation in a satisfactory degree could be used to estimate the concentration of uranium at any given time. Then a predictive model of ash concentration in time intervals follows the equation:

$$[U^{IV}] = \frac{1}{\frac{1}{[U^{IV}]_0} + kt} \tag{5}$$

The uranium mass balance can be expressed as:

$$[U]_{total} = [U^{IV}] + [U^{VI}] \tag{6}$$

Total uranium concentration can also be defined as the initial concentration of uranium introduced into the system in ash. Therefore, in relation to previous assumptions, this value refers to the concentration of uranium at the IV oxidation stage at time t = 0. Therefore, by combining the two above equations (5) and (6), we get a function that expresses the concentration of uranium in the liquid phase (U^{VI}):

$$[U^{VI}] = [U^{IV}]_0 - \frac{1}{\frac{1}{[U^{IV}]_0} + kt} \tag{7}$$

The equation can be rearranged in a simpler form. The denominator of the expression can be written:

$$\frac{1}{[U^{IV}]_0} + kt = \frac{1 + [U^{IV}]_0 kt}{[U^{IV}]_0} \tag{8}$$

Then:

$$\frac{1}{\frac{1}{[U^{IV}]_0} + kt} = \frac{[U^{IV}]_0}{1 + [U^{IV}]_0 kt} \tag{9}$$

Substituting this into the original equation, it is obtained:

$$[U^{VI}] = [U^{IV}]_0 - \frac{[U^{IV}]_0}{1 + [U^{IV}]_0 kt} \tag{10}$$

Or

$$[U^{VI}] = [U^{IV}]_0 \left(1 - \frac{1}{1 + [U^{IV}]_0 kt}\right) \tag{11}$$

where:

$[U^{VI}]$ – is uranium concentration in liquid phase (mg· kg^{-1})

$[U^{IV}]_0$ – is uranium initial concentration of ash (mg· kg^{-1})

k – is the second-order rate constant (k = $3.58.10^{-4}$ ±$0.31.10^{-4}$ kg mg^{-1}·min^{-1})

t – is time (min)

3.3. Diffusion through the membrane

The kinetics of uranium diffusion through membranes was studied in two cell systems separated by membranes. The experiment began with the addition of a known amount of uranium to cell 1, followed by the measurement of the concentration in cell 2 over time. The experimental result was the increase in the concentration in the cell behind the membrane (cell 2) as shown in Fig. 7. All data sets (A,B,C) come from repeating the experiment and follow a similar trend characterised by a rapid initial increase in uranium concentration followed by a gradual approach to equilibrium. The curve follows a characteristic asymptotic behaviour, indicating a diffusion-driven transport process, where the flux decreases over time as the concentration gradient decreases. The barrier of maximum concentration is marked in the figure as the equilibrium concentration. Approximately 47 h were needed to achieve that point of full diffusion. This practically means equal concentration between cells and equilibrium between the transition of uranium from cell 1 to 2 and cell 2 to 1. Under normal pressure, which was observed during the conducted experiment, the process can be considered complete. The relation shown in the figure is well described by a natural logarithm function. Then, it is worth mentioning that up to the 90 % level, the process took 16.7 h less time and 50 % of the uranium passed the membrane in just 6 h. The results confirm that the uranium diffusion process is governed by the Fick law and follows simple passive diffusion patterns (Cussler, 2009).

Fick's law in its first form describes the flux of a substance J (the amount of substance carried by a unit area per unit time), and according to uranium diffusion:

$$J_U = -D\frac{dU}{dx} \tag{12}$$

where:

J_U - is the diffusion flux of uranium.

D - is the diffusion coefficient.

$\frac{dU}{dx}$ is the concentration gradient with respect to width (x) of membrane

Integrating the equation from 0 to the membrane thickness x and for the concentration gradient U_{in} to U_{out}, the equation will take the form of the following:

$$J_U = \frac{D}{x}(U_{in} - U_{out}) \tag{13}$$

Relating the concentration differences as the uranium gradient ΔU and including that D/x in the literature is taken as a coefficient of permeability (P), we obtain a linear function (Cussler, 2009):

$$J_U = P\Delta U \tag{14}$$

According to this, Fig. 8 shows the diffusion flux plotted against the uranium concentration gradient between cells. The data points are

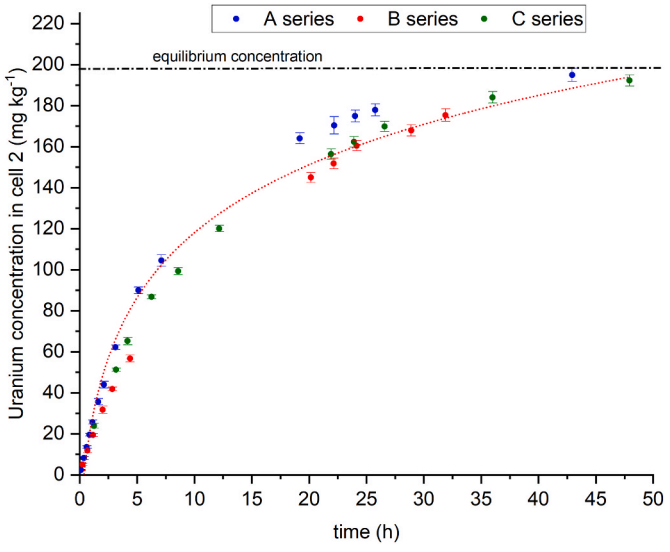

Fig. 7. Changes of uranium concentration (cell 2) in diffusion experiment.

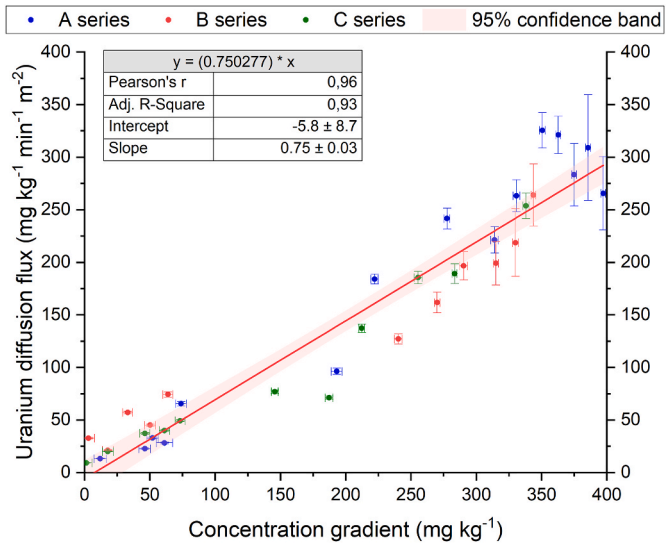

Fig. 8. Diffusion flux plotted against the uranium concentration gradient between cells.

categorised into series, with a linear regression line fitted to all data. The adjusted R-square value further supports the robustness of the linear model. The slope of the function is equal to the permeability coefficient and is 0.75 ± 0.3 cm min $^{-1}$. The intercept of the regression line is −5.8 ± 8.7, which is not significantly different from zero, suggesting that diffusion is negligible in the absence of a concentration gradient. This is consistent with the derived form of the uranium diffusion flux.

Deriving a predictive model for the concentration in cell 2, the diffusion flux was related to the rate of change of the amount of substance in chamber 2:

$$\frac{dU_{out}}{dt} = P(U_{in} - U_{out}) \tag{15}$$

Solving this differential equation with the assumption of concentration = 0 at t = 0 in cell 2 for a closed system with equal volumes results in the following approximate solution:

$$U_{out(t)} = U_{in\ (t=0)}\left(1 - e^{-Pt}\right) \tag{16}$$

where:

U_{out} – uranium concentration in outer cell.

$U_{in\ (t\ =\ 0)}$ – uranium concentration in the inner cell in time = 0.

P - permeability coefficient P = 0.75 ± 0.3

t-time.

In cell 1 (before membrane) the uranium concentration can be calculated by analogy:

$$\frac{dU_{in}}{dt} = P(U_{out} - U_{in}) \tag{17}$$

an approximate solution of the differential equation is:

$$U_{in(t)} = U_{in\ (t=0)}\left(1 - e^{-Pt}\right) \tag{18}$$

When the approximate solution is applicable to the conditions of the experiment, the differential form is the essence for the method of uranium extraction in a membrane system proposed in this work. This is due to the variable concentration over time, which is related to its gain in the oxidation of uranium from ash.

Equations (11), (15) and (17) represent a key achievement for the predictive model, which is an important step in the design of uranium leaching plants based on the proposed method. It allows for the prediction of uranium concentration over time and the time required to reach the assumed recovery level. This will be particularly important for optimising the installation on a larger than laboratory scale.

Although membrane diffusion experiments were conducted using a simplified model solution containing only uranyl ions in nitric acid, it is important to consider the complexity of the actual leachates obtained from coal fly ash. Coal fly ash is a heterogeneous industrial by-product composed primarily of oxides of silicon, aluminium, and iron, with additional contributions from calcium, magnesium, sodium, potassium, and trace elements. Typically, 90–99 % of its composition consists of Si, Al, Fe, Ca, Mg, Na, and K, with SiO_2 and Al_2O_3 forming the dominant matrix components (Adriano et al., 1980; Jala and Goyal, 2006).

There is the possibility that the presence of coexisting metal ions in real leachates may influence the membrane transport of uranium by altering the overall diffusion environment.

In addition, the long-term durability and reusability of the membrane were not assessed in this work. Since the focus was on short-term, single-use experiments, no decline in membrane performance was observed. However, for the potential future implementation of this method, a systematic evaluation of the stability of the membrane, resistance to chemical degradation, and the possibility of repeated use will be necessary to assess the operational feasibility under extended or cyclic conditions.

4. Conclusion

The experiments carried out in this study demonstrated a useful methodology for the separation and recovery of uranium from calcined ash, the adopted leaching approach showing high effectiveness and an average recovery of 96.7 %. Two kinetic models were applied to describe the process: second-order reaction kinetics for the leaching step and simple diffusion for the transport of uranium through the membrane. This dual-model approach provides valuable insight into the physical mechanisms underlying the system and enables the development of predictive tools for future scaling and process optimisation. Key experimental parameters, including the permeability coefficient and leaching rate constant, were determined and will serve as the basis for the design of operations in subsequent stages of industrial application. The next step of the experiment can be the verification of the effects of matrix complexity on the behaviour of uranium diffusion in practical applications. Further validation of the proposed diffusion model is planned in an integrated system that combines coal ash leaching with membrane-based separation to account for the influence of the full chemical matrix and coexisting ions on uranium transport. In general, this study supports the sustainable development of nuclear energy by exploring alternative sources of uranium for fuel production. The proposed membrane-assisted method addresses key challenges associated with the complex physical nature of ash residues, and its further refinement may contribute to improved efficiency and circularity in the nuclear fuel cycle.

CRediT authorship contribution statement

Filip Jedrzejek: Writing – review & editing, Writing – original draft, Visualization, Methodology, Funding acquisition, Formal analysis, Data curation, Conceptualization. **Weronika Mendera:** Writing – review & editing, Methodology, Investigation, Conceptualization. **Katarzyna Szarlowicz:** Writing – review & editing, Validation, Supervision, Funding acquisition. **Niklas Heiss:** Writing – review & editing, Methodology. **Ulrich W. Scherer:** Writing – review & editing, Methodology.

Funding

This work was supported by The National Science Centre (POLAND), MINIATURA 7 project ID: 2023/07/X/ST8/01116.

Declaration of competing interest

The authors declare the following financial interests/personal relationships which may be considered as potential competing interests: Filip Jedrzejek reports financial support was provided by National Science Centre Poland. If there are other authors, they declare that they have no known competing financial interests or personal relationships that could have appeared to influence the work reported in this paper.

Data availability

The raw data were made available in the repository under the Creative Commons BY 4.0 licence: https://doi.org/10.58032/AGH/XLAPWE

References

Adriano, D.C., Page, A.L., Elseewi, A.A., Chang, A.C., Straughan, I., 1980. Utilization and disposal of fly ash and other coal residues in terrestrial ecosystems: a review. J. Environ. Qual. 9, 333–344.

Ahmed, U.A.Q., Wagner, N.J., Joubert, J.A., 2020. Quantification of U, Th and specific radionuclides in coal from selected coal fired power plants in South Africa. PLoS One 15, e0229452.

Arbuzov, S.I., Volostnov, A.V., Rikhvanov, L.P., Mezhibor, A.M., Ilenok, S.S., 2011. Geochemistry of radioactive elements (U, Th) in coal and peat of northern Asia (Siberia, Russian Far East, Kazakhstan, and Mongolia). Int. J. Coal Geol. 86, 318–328.

Berger, P., 1988. Etude du mécanisme de la dissolution par oxydoréduction chimique et électrochimique des bioxydes d'actinides (UO2, NpO2, PuO2, AmO2. en milieu aqueux acide. Paris 6.

Cussler, E.L., 2009. Diffusion: Mass Transfer in Fluid Systems, 3 ed. Cambridge University Press, Cambridge.

Delegard, C.H., Schmidt, A.J., 2009. Uranium Metal Reaction Behavior in Water, Sludge, and Grout Matrices. United States.

Ebaid, Y., 2015. USE OF GAMMA-RAY SPECTROMETRY FOR URANIUM ISOTOPIC ANALYSIS IN ENVIRONMENTAL SAMPLES.

Edenhofer O, P.-M.R., Sokona, Y., 2011. Renewable Energy Sources and Climate Change Mitigation: Special Report of the Intergovernmental Panel on Climate Change. Cambridge University Press, Cambridge.

Fidanchevski, E., Angjusheva, B., Jovanov, V., Murtanovski, P., Vladiceska, L., Aluloska, N.S., Nikolic, J.K., Ipavec, A., Šter, K., Mrak, M., Dolenec, S., 2021. Technical and radiological characterisation of fly ash and bottom ash from thermal power plant. J. Radioanal. Nucl. Chem. 330, 685–694.

Finkelman, R.B., 1994. Modes of occurrence of potentially hazardous elements in coal: levels of confidence. Fuel Process. Technol. 39, 21–34.

Fournier, S., 2000. Étude de la dissolution des oxydes mixtes (U, Pu) O2 à forte teneur en plutonium, vol. 2. Montpellier.

Gao, J., Chen, J., Lv, H., Liao, S., Feng, X., Yan, Y., Xue, Y., Tian, G., Ma, F., 2023. Electrocatalytic and green system coupling strategy for simultaneous recovery and purification of uranium from uranium-containing wastewater. J. Environ. Manag. 342, 118151.

Harrison, K., 2018. The politics of carbon pricing. Nat. Clim. Change 8, 852-852.

Herrmann, B., 1984. Dissolution of Unirradiated UO 2-pellets in Nitric Acid. Kernforschungszentrum Karlsruhe GmbH, Germany.

Hower, J.C., Ruppert, L.F., Eble, C.F., 1999. Lanthanide, yttrium, and zirconium anomalies in the fire clay coal bed, Eastern Kentucky. Int. J. Coal Geol. 39, 141–153.

IAEA, 2003. Extent of Environmental Contamination by Naturally Occurring Radioactive Material (NORM) and Technological Options for Mitigation. INTERNATIONAL ATOMIC ENERGY AGENCY, Vienna.

IAEA, 2015. Naturally Occurring Radioactive Material (NORM VII). INTERNATIONAL ATOMIC ENERGY AGENCY, Vienna.

IAEA, 2023. Nuclear Energy in Climate Resilient Power Systems. INTERNATIONAL ATOMIC ENERGY AGENCY, Vienna.

Ikeda, Y., Yasuike, Y., Takashima, Y., Park, Y.-Y., Asano, Y., Tomiyasu, H., 1993. 17O NMR study on dissolution reaction of UO2 in nitric acid mechanism of electron transfer. J. Nucl. Sci. Technol. 30, 962–964.

Intergovernmental Panel on Climate, C, 2015. Climate Change 2014: Mitigation of Climate Change: Working Group III Contribution to the IPCC Fifth Assessment Report. Cambridge University Press, Cambridge.

Jala, S., Goyal, D., 2006. Fly ash as a soil ameliorant for improving crop production—a review. Bioresour. Technol. 97, 1136–1147.

Jędrzejek, F., Szarłowicz, K., 2024. Evaluation and reduction of background interference caused by airborne particles in gamma spectrometry measurements. Measurement 232, 114730.

Jędrzejek, F., Szarłowicz, K., Stobiński, M., 2022. A geological context in radiation risk assessment to the public. Int. J. Environ. Res. Publ. 19, 18.

Karamanis, D., Vardoulakis, E., 2012. Application of zeolitic materials prepared from fly ash to water vapor adsorption for solar cooling. Appl. Energy 97, 334–339.

Mahur, A.K., Kumar, R., Sengupta, D., Prasad, R., 2008. Estimation of radon exhalation rate, natural radioactivity and radiation doses in fly ash samples from Durgapur thermal power plant, West Bengal, India. J. Environ. Radioact. 99, 1289–1293.

Marc, P., Magnaldo, A., Vaudano, A., Delahaye, T., Schaer, É., 2017. Dissolution of uranium dioxide in nitric acid media: what do we know? EPJ Nucl. Sci. Technol. 3.

Mishra, M., Sahu, S.K., Mangaraj, P., Beig, G., 2023. Assessment of hazardous radionuclide emission due to fly ash from fossil fuel combustion in industrial activities in India and its impact on public. J. Environ. Manag. 328, 116908.

Monnet, A., Percebois, J., Gabriel, S., 2015. Assessing the potential production of uranium from coal-ash milling in the long term. Resour. Policy 45, 173–182.

Muellner, N., Arnold, N., Gufler, K., Kromp, W., Renneberg, W., Liebert, W., 2021. Nuclear energy - the solution to climate change? Energy Policy 155, 112363.

NEA, 2014. Managing Environmental and Health Impacts of Uranium Mining. Paris.

Nian, V., 2016. Analysis of interconnecting energy systems over a synchronized life cycle. Appl. Energy 165, 1024–1036.

Olkuski, T., 2008. Zawartość Uranu i Toru W Węglach Polskich i Amerykańskich.

Peters, M., Fudge, S., High-Pippert, A., Carragher, V., Hoffman, S.M., 2018. Community solar initiatives in the United States of America: comparisons with – and lessons for – the UK and other European countries. Energy Policy 121, 355–364.

Richardson, J.F., Harker, J.H., Backhurst, J.R., 2002. Chapter 10 - leaching. In: Richardson, J.F., Harker, J.H., Backhurst, J.R. (Eds.), Chemical Engineering, fifth ed. Butterworth-Heinemann, Oxford, pp. 502–541.

Saunders, J.A., Pivetz, B.E., Voorhies, N., Wilkin, R.T., 2016. Potential aquifer vulnerability in regions down-gradient from uranium in situ recovery (ISR) sites. J. Environ. Manag. 183, 67–83.

Smolka-Danielowska, D., 2010. Rare earth elements in fly ashes created during the coal burning process in certain coal-fired power plants operating in Poland – upper Silesian industrial region. J. Environ. Radioact. 101, 965–968.

Stobiński, M., Jędrzejek, F., Kubica, B., 2018. Preliminary studies on the spatial distribution of artificial Cs and natural gamma radionuclides in the region of the Ojców National Park, Poland. Nukleonika 63, 105–111.

Su, Q., Zhang, X.W., Li, M., Zhang, Y., Li, S.F., 2014. Separation and characteristics of colloid in leaching residual ores column of a hard uranium ores. Adv. Mater. Res. 953–954, 1008–1011.

Sun, Y., Qi, G., Lei, X., Xu, H., Wang, Y., 2016. Extraction of uranium in bottom ash derived from high-germanium coals. Procedia Environ. Sci. 31, 589–597.

Taylor, G.H., 1979. Chapter 8 biogeochemistry of uranium minerals. In: Trudinger, P.A., Swaine, D.J. (Eds.), Studies in Environmental Science. Elsevier, pp. 485–514.

Vance, R., 2016. 4 - uranium resources. In: Hore-Lacy, I. (Ed.), Uranium for Nuclear Power. Woodhead Publishing, pp. 77–97.

Verma, M., Loganathan, V.A., 2025. Uranium concentration from acidic mine effluent using forward osmosis. J. Environ. Manag. 376, 124340.

Walencik-Łata, A., Smołka-Danielowska, D., 2020. 234U, 238U, 226Ra, 228Ra and 40K concentrations in feed coal and its combustion products during technological processes in the upper Silesian industrial region, Poland. Environ. Pollut. 267, 115462.

Zielinski, R.A., Finkelman, R.B., 1997. Radioactive Elements in Coal and Fly Ash: Abundance, Forms, and Environmental Significance, Fact Sheet. Reston, vol. A.

Životić, D., Gržetić, I., Lorenz, H., Simić, V., 2008. U and Th in some brown coals of Serbia and Montenegro and their environmental impact. Environ. Sci. Pollut. Control Ser. 15, 155–161.